INTERFACE CURRENT NODAL FORMULATION OF SIMPLIFIED P2 EQUATIONS IN MULTI-DIMENSIONAL HEXAGONAL GEOMETRY

Taek Kyum Kim, Young-Jin Kim, and Young-Il Kim
Korea Atomic Energy Research Institute
P.O. Box 105, Yousung-gu, Teajeon-city, 305-600, KOREA
tkkim@kaeri.re.kr

ABSTRACT

An interface current nodal formulation was developed for the solution of the multi-group simplified P_2 (SP_2) equation in hexagonal geometry and has been incorporated in the framework of the conventional nodal diffusion equations. By introducing the SP_2 constant α and the SP_2 flux ζ, we can formulate the nodal SP_2 equations with minimum modification of the conventional diffusion nodal equations and make it possible to use the conventional numerical schemes, i.e., fission source iteration accelerated by coarse-mesh rebalancing method. But, the relationship between the surface-averaged flux and partial currents of the SP_2 approximation gives rise to additional term in the response matrix equations. Numerical calculations showed that, in the LMR problems, the SP_2 nodal solutions reduced the error of the multiplication factor up to 50 % and there were conspicuous improvements for estimating the region-averaged fluxes in the non-dense or blanket regions with higher neutron energies. However, we could not find any merit and demerit in the LWR problems because there were few non-dense regions and the higher energy effects were already condensed into the two-group cross sections. Since the SP_2 nodal equations required the computation of the surface-averaged sources additionally, the total computing time of the SP_2 nodal was increased and that may became a burden in the large size problems.

1. INTRODUCTION

The Simplified P_n (SP_n) equations were originally proposed by Gelbard to deal with the complexity of the general P_n equations[1-3]. The goal of SP_n method is to obtain a relatively inexpensive approximation to the transport equations that contains most of the transport physics lacking in diffusion theory. Numerous studies have been performed to investigate the accuracy of the SP_n equations, and confirmed that SP_n equations were significantly more accurate than diffusion equations but with almost the same computational efforts.[4-9] Nevertheless, the lack of theoretical background of the SP_n equations had obstructed the widespread usages of that. Recently, Lasen et al.[10,11] provided the theoretical background to the SP_n equations and showed that the SP_n equations could be understood as asymptotic correction to P_1 theory in optically thick and scattering dominated regions. These theoretical backgrounds are consistent with the general observation of researchers who have experimented numerically with SP_n equations.[4,8,9,11]

According to the previous researches for the SP_n equations, we might expect higher accurate solution from the SP_n equations than the diffusion equations and selected the SP_n equations to improve the accuracy of the Liquid Metal Rector (LMR) core design code system.[12,13] At the first stage, we used the SP_2 equations because the SP_2 equations can be implemented by minimum modifications of the conventional diffusion equations with an improved accuracy. Although it is true that the SP_2 equations are analogue to the P_1 equations, the existence of the P_2 flux gives rise to the different relationships between the P_1 and SP_2 approximations. For example, the relation between the partial currents and the surface averaged fluxes at the internal interfaces, the boundary conditions at the external surfaces, etc. So, in order to implement the scheme of a nodal expansion method with the SP_2 equations, some modifications of the conventional nodal diffusion equations and additional computation efforts are required to obtain the SP_2 nodal equations. In this paper, we describe the mathematical development and numerical solutions of the multi-group SP_2 equations. Specially, section 2 and 3 discuss the derivations of the multi-group SP_2 equations and the SP_2 nodal equations, respectively. Section 4 describes the numerical scheme to solve these nodal equations. Section 5 provides the numerical results by comparison with the solutions of a discrete ordinate transport method or the results of a critical experiment. And then, we write the conclusion in the section 6.

2. MULTI-GROUP SIMPLIFIED P_2 EQUATIONS

SP_n equations can be derived by the replacement of the one-dimensional operators into multi-dimensional operators at the one-dimensional P_n equations[1,11]. The multi-group SP_2 equations for a homogeneous node k are composed of three equations:

$$\vec{\nabla}\cdot\vec{\phi}^{k}_{1g}(\vec{r})+\Sigma^{k}_{rg}\phi^{k}_{0g}(\vec{r})=Q^{k}_{g}(\vec{r}), \tag{2.1.a}$$

$$\frac{2}{3}\vec{\nabla}\cdot\phi^{k}_{2g}(\vec{r})+\frac{1}{2}\vec{\nabla}\phi^{k}_{0g}(\vec{r})+\Sigma^{k}_{tr1g}\vec{\phi}^{k}_{1g}(\vec{r})=0, \tag{2.1.b}$$

$$\frac{2}{5}\vec{\nabla}\cdot\vec{\phi}^{k}_{1g}(\vec{r})+\Sigma^{k}_{tr2g}\phi^{k}_{2g}(\vec{r})=0, \tag{2.1.c}$$

where

$$Q^{k}_{g}(\vec{r})=\sum_{g'\neq g}^{G}\Sigma^{k}_{sgg'}\phi^{k}_{0g'}(\vec{r})+\frac{\chi^{k}_{g}}{k}\sum_{g'=1}^{G}\upsilon\Sigma^{k}_{fg'}\phi^{k}_{0g'}(\vec{r}), \tag{2.2.a}$$

$$\Sigma^{k}_{trng}=\Sigma^{k}_{tg}-\Sigma^{k}_{sng},\ n=1,2, \tag{2.2.b}$$

$$\Sigma^{k}_{rg}=\Sigma^{k}_{tg}-\Sigma^{k}_{s0gg}, \tag{2.2.c}$$

and other notations are conventional (see Ref. 14-16). We can reduce the Eqs. (2.1) into one equation with an unknown, ϕ_{0g},

$$-\vec{\nabla}\cdot D\vec{\nabla}\cdot\{(1+\alpha\Sigma_r)\phi-\alpha Q\}+\Sigma_r\phi=Q, \tag{2.3}$$

,where

$$\phi_1=-D\vec{\nabla}\cdot\{(1+\alpha\Sigma_r)\phi-\alpha Q\}, \tag{2.4}$$

$$\phi_2=\frac{1}{2}\alpha\{\Sigma_r\phi-Q\}, \tag{2.5}$$

$$D=1\big/3\Sigma_{tr1}, \tag{2.6}$$

$$\alpha=4\big/5\Sigma_{tr2}. \tag{2.7}$$

For simplicity, we omitted the sub- and super-script denoting the group and node index in the above equations and ϕ denotes the scalar flux, ϕ_0. Since $\vec{\phi}_1$ is understood as the current, it is often represented by $\vec{J}$. The Eq. (2.3) has a different form the conventional diffusion equations because of the existence of α. In order to transfer the SP_2 equations

into the form of the conventional diffusion equations, we define the SP_2 flux, ζ,

$$\zeta = (1+\alpha\Sigma_r)\phi - \alpha Q, \tag{2.8}$$

and insert it into Eq. (2.3), and then we can get the diffusion like SP_2 equation,

$$-\nabla \cdot D\nabla \cdot \zeta + \Sigma_r^s \zeta = Q^s, \tag{2.9}$$

where

$$\Sigma_r^s = \frac{\Sigma_r}{1+\alpha\Sigma_r}, \tag{2.10.a}$$

$$Q^s = (1-\alpha\Sigma_r^s)Q. \tag{2.10.b}$$

In the above equations, if α goes to zero, ζ, Q^s, and Σ_r^s become ϕ, Q, and Σ_r, respectively, and Eq. (2.9) is identical with the diffusion equation. So, we call it 'a SP_2 factor'. In the SP_2 approximations, the relation between the surface-averaged flux, $\overline{\phi}_{us}$, and the surface-averaged partial currents at the right($s = r$) and left($s = l$) normal surfaces to the direction u is

$$\overline{\phi}_{us} = 2(J_{us}^{out} + J_{us}^{in}) - \frac{5}{8}\alpha(\Sigma_r \overline{\phi}_{us} - \overline{Q}_{us}), \tag{2.11}$$

or

$$\overline{\zeta}_{us} = 2\kappa_3(J_{us}^{out} + J_{us}^{in}) + \kappa_4 \overline{Q}_{us}, \tag{2.12}$$

where

$$\kappa_3 = \frac{8(1+\alpha\Sigma_r)}{8+5\alpha\Sigma_r}, \tag{2.13}$$

$$\kappa_4 = -\frac{3\alpha}{(8+5\alpha\Sigma_r)}. \tag{2.14}$$

In Eqs. (2.11) and (2.12), $\overline{Q}_{us}$ denotes the surface-averaged source and J_{us}^{out}, J_{us}^{in} correspond to the surface-averaged outgoing and incoming partial current, respectively. We can specify the boundary condition of the general form

$$a\phi(\vec{r}) - 2b\hat{e}_s \cdot \vec{J}(\vec{r}) + cQ(\vec{r}) = 0, \quad \vec{r} \in S_b, \tag{2.15}$$

at the external boundary surface, S_b, with the it's normal vector, $\hat{e}_s$. Standard boundary

conditions (e.g. zero flux, vacuum boundary condition) are obtained via appropriate specification of the constants a, b, and c. For examples, the incoming partial current at the external vacuum boundary surface is

$$J_{us}^{in} = \left(\frac{1-2\beta}{1+2\beta}\right) J_{us}^{out} + \frac{5}{16}\left(\frac{1-2\beta}{1+2\beta}\right)\alpha \overline{Q}_{us}, \tag{2.16}$$

where

$$\beta = \frac{16\gamma + 5\alpha\Sigma_r}{16 + 10\alpha\Sigma_r}, \tag{2.17}$$

and γ is a constant determined by the conventional "Marshak boundary condition" of the P_1 approximation.[16] The above boundary condition, Eq. (2.16), has a different form with the conventional "Marshak boundary condition" of the P_1 approximation[16] because of the existence of the surface-averaged source. But, if α goes to zero, Eq. (2.16) is identical with the conventional "Marshak boundary condition" of the P_1 approximation.

3. NODAL EXPANSION METHOD FOR THE SIMPLIFIED P_2 EQUATIONS

Because we deal with a homogeneous node and the SP_2 flux(ζ) is defined by the linear combination of scalar fluxes shown in Eq. (2.8), we can define all nodal parameters of SP_2 equations equivalently with the nodal parameters of the diffusion equations. And the nodal expansion method (NEM) can be easily applied to the SP_2 equations. Thus, the form of the nodal balance and the flux moment equations of nodal SP_2 equations are same with those of the nodal diffusion equations except for the replacement of the scalar flux and the removal cross-section with the SP_2 fluxes and the newly defined removal cross-section shown in Eq. (2.8) and (2.10.a), respectively. In order to solve the nodal scheme of the SP_2, we must know the node-averaged flux, surface-averaged fluxes, surface-averaged currents, and first order flux moments. But it is possible to represent the surface-averaged fluxes and currents by using the surface-averaged partial currents, the total unknowns per node per group in the nodal scheme of the SP_2 equations become 13, i.e., one node averaged flux, four first order flux moments, and eight surface-averaged outgoing partial currents which are the incoming partial currents for the neighboring nodes. These situations are similar with the nodal

scheme of diffusion equations. But there is one difference feature in determining the surface-averaged fluxes from the surface-averaged partial currents. Eqs. (2.11) and (2.12) show the relation between the surface-averaged flux and the surface-averaged partial currents. In the diffusion or P_1 approximation, κ_3 and κ_4 become unity and zero, respectively. But, not only these values are different but also the surface-averaged source term is added in the SP_2 approximation. Therefore, these differences require the additional computations of the surface-averaged sources and modifications of the conventional response matrix equations. By the analogue manner of reference 14, we obtain the response matrix equations as following:

$$\mathbf{A}\mathbf{J}^{out} = \mathbf{B}(\mathbf{Q}-\mathbf{L}) + \mathbf{C}\mathbf{J}^{in} + \mathbf{B}_s\mathbf{Q}_s, \tag{3.1}$$

where matrix **B** and vector **Q-L** are equivalent to that defined in the nodal scheme of the diffusion equations but matrix **A** and **C** are slightly different because of the existence of κ_3 in (2.12). The last term of Eq. (3.1) is originated in the relation between the surface-averaged flux and the surface-averaged partial currents and they are defined by

$$\mathbf{B}_s \equiv \begin{pmatrix} b_{xyr} & 0 & 0 & b_{xyl} & 0 & 0 & 0 & 0 \\ 0 & b_{xyr} & 0 & 0 & b_{xyl} & 0 & 0 & 0 \\ 0 & 0 & b_{xyr} & 0 & 0 & b_{xyl} & 0 & 0 \\ b_{xyl} & 0 & 0 & b_{xyr} & 0 & 0 & 0 & 0 \\ 0 & b_{xyl} & 0 & 0 & b_{xyr} & 0 & 0 & 0 \\ 0 & 0 & b_{xyl} & 0 & 0 & b_{xyr} & 0 & 0 \\ 0 & 0 & 0 & 0 & 0 & 0 & b_{zr} & b_{zl} \\ 0 & 0 & 0 & 0 & 0 & 0 & b_{zl} & b_{zr} \end{pmatrix}, \tag{3.2}$$

$$\mathbf{Q}_s \equiv col.\left(\overline{Q}_{xr} \quad \overline{Q}_{ur} \quad \overline{Q}_{ul} \quad \overline{Q}_{xl} \quad \overline{Q}_{ul} \quad \overline{Q}_{vl} \quad \overline{Q}_{zr} \quad \overline{Q}_{zl}\right), \tag{3.3}$$

where

$$b_{xyr} = -\frac{1}{2}\kappa_4\tau_1, \tag{3.4.a}$$

$$b_{xyl} = -\frac{1}{2}\kappa_4\tau_2, \tag{3.4.b}$$

$$b_{zr} = -\frac{1}{2}\kappa_4\tau_{z1}, \tag{3.4.c}$$

$$b_{zl} = -\frac{1}{2}\kappa_4 \tau_{z2}, \tag{3.4.d}$$

and the constants $\tau_i (i = 1,2,z1,z2)$ are equivalent to the constants defined in the nodal scheme of diffusion equations and they are described in the reference 14. If the SP_2 factor, α, goes to zero, matrix $\mathbf{B}_s$ becomes a null matrix and matrix **A** and **C** are identical to the matrices defined in the nodal scheme of the diffusion equations. The final form of the response matrix equation is obtained by inverting **A** in Eq. (3.1) to yield

$$\mathbf{J}^{out} = \mathbf{P}(\mathbf{Q} - \mathbf{L}) + \mathbf{R}\mathbf{J}^{in} + \mathbf{S}\mathbf{Q}_s, \tag{3.5}$$

where

$$\mathbf{P} = \mathbf{A}^{-1}\mathbf{B}, \tag{3.6.a}$$
$$\mathbf{R} = \mathbf{A}^{-1}\mathbf{C}, \tag{3.6.b}$$
$$\mathbf{S} = \mathbf{A}^{-1}\mathbf{B}_s. \tag{3.6.c}$$

4. NUMERICAL SCHEME

Since the SP_2 nodal equations are analogue to the diffusion nodal equations, there are no problems to implement the conventional numerical methods, such as a fission source iteration procedure accelerated by coarse-mesh rebalancing method and red-black iterations[14]. At each outer iteration, the outgoing partial currents for each group are computed by solving the response matrix equations with the known group node-averaged and surface-averaged sources. In these procedures, the solutions are accomplished by sweeping the nodes in a four-color checkerboard ordering in a hexagon plane and a standard red-black checkerboard ordering to the axial planes. Then, the flux moments are computed. Once all energy groups have been processed, the outer iterations are accelerated using the coarse-mesh rebalance method. The outer iterations are terminated when some convergence criteria, e.g., eigenvalue, fission sources, etc., are satisfied. In comparison the computational effect between the diffusion and the SP_2 equations, there are two additional computations in the SP_2 equations. First one is to prepare some constants appeared in the SP_2 equations, e.g., α, $\kappa_{3,4}$ and Σ_r^s, etc. Second one is the computation of the surface-averaged sources to solver the response matrix equation, Eq. (3.1). And they may be a burden in the SP_2 nodal method because it is difficult to ignore these additional computations in the three-dimensional large size problems.

5. BENCHMARK CALCULATIONS

Numerical results are presented in this section for the several benchmark problems[17-21] and two series of the fast critical experiments.[22-25] Diffusion and SP_2 nodal results are compared by the reference S_n transport calculations in terms of the accuracy of multiplication factor, the respective spatial flux distributions and the computational effort required to achieve this accuracy. Generally, it is necessary to confirm the accuracy of the three-dimensional SP_2 nodal scheme by direct comparison with an accurate reference transport calculations for three-dimensional geometry. But, because we could not access three-dimensional transport code with an appropriate accuracy, we just compared the two-dimensional problems with the reference solutions of TWOHEX[26] with S_8 approximation, 24 triangles per hexagon. All calculations were performed on a PC with a Pentium-II processor.

5.1. SNR BENCHMARK PROBLEM

The two-dimensional SNR problems correspond to the “rods in” and “rod out” configurations, representing a horizontal slices taken through the upper and lower half part of core, respectively.[17] Table I and II show the results, where FDM solution means the Richardson extrapolation of DIF3D referred in reference 17. One can find that the eigenvalues of TWOHEX are always larger than those of the diffusion FDM solutions, which mainly result from transport theory effect found by other authors.[27,28] Same trend was occurred between the SP_2 and diffusion nodal calculations; that is to say, because the low-order SP_N solutions often catch up the transport effect in some degrees,[5,7] the eigenvalues of the SP_2 nodal calculations were lager than those of the nodal diffusion calculations. Therefore, the eigenvalues of SP_2 nodal were closer to the results of TWOHEX up to 80% than those of the diffusion nodal. The errors of the region-averaged fluxes were generally reduced in the SP_2 nodal calculations. Especially, the region-averaged fluxes in the regions of rod and follower were remarkable reduced, i.e., the SP_2 nodal underestimated maximum 4.5% in the follower region but the diffusion nodal overestimated maximum 7.3% in the rod region. These opposite signs of the errors between the SP_2 and diffusion calculations are found consistently in the reference 5.

Table I. Results of two-dimensional SNR problem.

Core	Group	Region	TWOHEX S8	Diffusion[1)]		SP2[1)]
				FDM	Nodal	Nodal
Rod-in	1	Inner	3.9959E+08	1.1	0.8	0.5
		Outer	2.2033E+08	-2.6	-2.1	0.2
		Radial Blanket	4.2106E+07	4.1	3.8	-2.6
		Rods	2.2607E+08	7.5	7.3	-2.3
		Followers	3.7732E+08	6.0	5.3	-4.0
	2	Inner	2.0041E+09	0.8	0.6	0.2
		Outer	9.7117E+08	-0.9	-0.7	-0.4
		Radial Blanket	3.2088E+08	-2.5	-1.5	-2.9
		Rods	1.0840E+09	2.7	2.4	-0.1
		Followers	2.1387E+09	1.0	0.8	0.2
	3	Inner	1.8100E+08	0.8	0.7	0.3
		Outer	8.0415E+07	-0.6	-0.7	-0.8
		Radial Blanket	4.3493E+07	-3.5	-1.4	-2.4
		Rods	7.3641E+07	1.9	0.7	-1.0
		Followers	2.2813E+08	0.0	0.8	1.2
	4	Inner	3.1766E+07	0.6	1.0	0.6
		Outer	1.1780E+07	-1.0	-0.9	-1.2
		Radial Blanket	1.1744E+07	-5.5	-2.6	-2.9
		Rods	6.4377E+06	2.6	-1.5	-2.9
		Followers	4.6872E+07	-2.3	-0.8	3.1
	effective k		1.13062	-0.59	-0.47	-0.09
	CPU time (sec)		113.7	-	1.0	1.2
Rod-out	1	Inner	3.3884E+08	1.0	0.8	0.7
		Outer	2.2932E+08	2.3	1.8	0.3
		Radial Blanket	4.3591E+07	4.8	4.4	-2.3
		Followers	2.7389E+08	5.0	4.6	-4.5
	2	Inner	1.8228E+09	0.6	0.5	0.2
		Outer	1.1011E+09	0.5	0.3	-0.3
		Radial Blanket	3.5611E+08	2.1	1.1	-2.6
		Followers	1.5524E+09	0.3	0.3	0.1
	3	Inner	1.7141E+08	0.6	0.4	0.2
		Outer	1.0074E+08	0.3	0.5	-0.8
		Radial Blanket	4.8958E+07	3.0	1.1	-2.2
		Followers	1.6384E+08	0.7	0.1	1.0
	4	Inner	3.1631E+07	0.4	0.4	0.3
		Outer	1.7030E+07	0.3	0.7	-1.2
		Radial Blanket	1.3467E+07	5.1	2.5	-2.8
		Followers	3.2495E+07	3.2	1.8	2.8
	effective k		1.22962	-0.44	-0.35	-0.19
	CPU time (sec)		112.4	-	0.9	1.0

1) Percent difference

5.2 BFS FAST CRITICAL EXPERIMENTS

As a part of the cooperation program between IPPE of Russia and KAERI, several critical experiments were performed in the BFS-1 critical facility for investigating the neutronics characteristics of metallic fast reactors.[22-35] There were two series critical assemblies, BFS-50's and BFS-70's, where metallic plutonium and uranium fuels were mounted, respectively. Table II and Figure 1 & 2 show the characteristics and the layout of critical assemblies.

Table II. Core characteristics of BFS critical experiment series

	BFS-55-1	BFS-55-2	BFS-73-1	BFS-75
Core 1	10% metallic Pu	10% metallic Pu-Zr	18.5% metallic U	15% metallic U-Zr
Core 2	-	10% metallic Pu	18.5% metallic U	20% metallic U-Zr
Radial blanket	depleted UO_2	depleted UO_2	depleted UO_2	depleted U^{238}/UO_2
Axial blanket	depleted U^{238}/UO_2	depleted U^{238}/UO_2	depleted UO_2	depleted UO_2
Pitch (cm)	5.1	5.1	5.1	5.1
Eq. Radius (cm)				
Core 1	56.1	37.5	50.0	25.5
Core 2	-	45.1	55.1	42.6
Radial blanket	99.5	99.5	91.1	91.1
Thickness (cm)				
Core	102.3	101.1	98.3	103.6
Axial Blanket	41.1	41.1	49.7	48.4

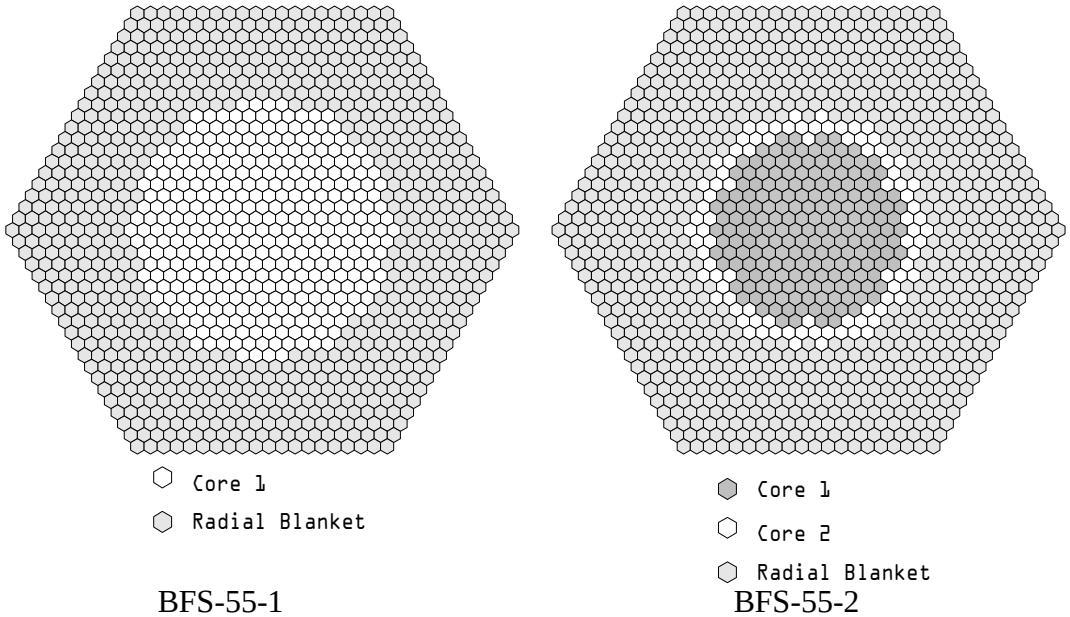

BFS-55-1 BFS-55-2

Figure 1. The Core Layout of BFS-50's Series Critical Assemblies

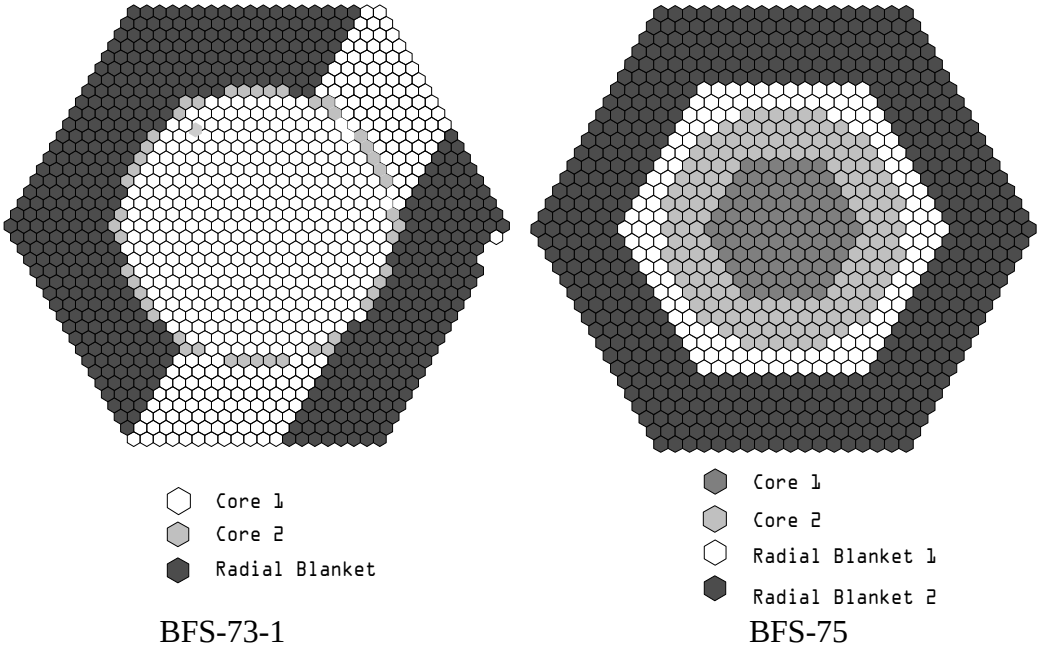

BFS-73-1 BFS-75

Figure 2. The Core Layout of BFS-70's Series Critical Assemblies

We calculated two- and three-dimensional geometries. The multiplication factors of three-dimensional geometries were compared with the measured ones and the two-dimensional results were compared with the solution of two-dimensional transport code, TWOHEX. In these calculations, we followed the standard LMR core design procedures with the K-CORE system of KAERI.[12,13] The 9 group effective cross sections were prepared in ISOTXS format and they were provided for the SP_2, diffusion nodal scheme and TWOHEX code. Table III shows the multiplication factors and computation time of three-dimensional calculations.

Table III. Multiplication factors from three-dimensional calculations (CPU time, sec)

Core	Multiplication factor			Computation time (sec)	
	Measured	Diffusion[1)]	SP_2[1)]	Diffusion	SP_2
BFS-55-1	1.00068 ± 17 pcm[2)]	-220 pcm	51 pcm	533	1131
BFS-55-2	1.00026 ± 15 pcm	-370 pcm	- 22 pcm	481	844
BFS-73-1	1.00080 ± 28 pcm	- 242 pcm	- 32 pcm	146	269
BFS-75	1.00134 ± 28 pcm	- 242 pcm	17 pcm	441	831

1) difference with measured value in pcm
2) pcm = 1.0E-05.

The diffusion nodal underestimates the multiplication factors consistently and the differences of the multiplication factors of the diffusion nodal are bigger than those of SP_2 nodal. Although it is liable to be misunderstood to directly compare the accuracy of three-dimensional SP_2 nodal because of the measurement uncertainties in these experiments, the multiplication factors estimated by the SP_2 nodal are closer to the measured values. However, the SP_2 nodal scheme consumed more computation time up to two times than diffusion nodal scheme because of the additional computations for obtaining the surface-averaged sources. Table IV and V show the results of two-dimensional calculations of BFS-50's and BFS-70's series, respectively.

Table IV. Results of two-dimensional BFS-55-1 and BFS-55-2 critical assemblies

Group	Region	BFS-55-1			BFS-55-2		
		TWOHEX	Diffusion[1)]	SP2[1)]	TWOHEX	Diffusion	SP2
1	Core 1	1.3479E+07	-4.3	-3.5	6.1365E+06	1.3	-2.3
	Core 2				1.0691E+06	13.1	3.0
	Radial blanket	1.3159E+06	9.0	0.0	1.6986E+07	-3.5	-2.5
2	Core 1	3.0197E+08	0.2	0.7	1.3068E+08	3.0	1.3
	Core 2				2.1533E+07	11.2	3.9
	Radial blanket	3.1126E+07	7.4	1.9	3.5879E+08	-0.4	0.2
3	Core 1	6.0432E+08	-0.4	-0.1	2.1396E+08	0.1	0.6
	Core 2				6.0624E+07	6.8	0.9
	Radial blanket	7.4912E+07	3.9	0.8	4.2708E+08	-0.6	-0.2
4	Core 1	1.0179E+09	-0.2	-0.1	2.6371E+08	-0.8	-0.5
	Core 2				1.0750E+08	3.5	-0.6
	Radial blanket	1.4314E+08	2.3	0.2	3.7532E+08	-0.6	-0.3
5	Core 1	8.6251E+08	-0.4	-0.3	1.8745E+08	-0.6	-0.9
	Core 2				8.4260E+07	2.1	-1.1
	Radial blanket	1.7708E+08	1.9	0.2	2.4927E+08	-0.6	-0.4
6	Core 1	4.7533E+08	-0.2	-0.3	1.1107E+08	0.7	-0.7
	Core 2				5.2161E+07	0.9	-1.4
	Radial blanket	1.6070E+08	1.5	0.0	1.7701E+08	-0.6	-0.3
7	Core 1	2.6822E+08	-0.1	-0.3	7.1293E+07	1.6	-0.1
	Core 2				2.5004E+07	0.7	-1.0
	Radial blanket	1.1703E+08	0.9	-0.4	1.4539E+08	-0.6	-0.3
8	Core 1	6.1789E+07	0.0	-0.4	3.6129E+07	2.3	-0.1
	Core 2				7.7011E+06	-0.3	-0.8
	Radial blanket	5.7951E+07	0.3	-0.7	1.1997E+08	-0.5	-0.2
9	Core 1	3.6276E+07	0.1	-0.3	8.8232E+07	2.5	-0.3
	Core 2				1.2297E+07	-2.6	-0.1
	Radial blanket	4.3029E+07	-0.9	-1.5	4.5686E+08	-0.5	-0.1
K-eff		1.07523	-0.26	-0.13	1.14941	-0.32	-0.15
CPU		1214.8	2.8	5.1	1234.8	3.5	5.3

1) Percent difference

Table V. Results of two-dimensional BFS-73-1 and BFS-75 critical assemblies

group	region	BFS-73-1			BFS-75		
		TWOHEX	Diffusion[1)]	SP2[2)]	TWOHEX	Diffusion	SP2
1	Core 1	8.7013E+06	-0.9	-0.5	1.3829E+07	1.8	1.0
	Core 2	4.4119E+06	-4.1	5.0	1.0231E+07	-2.1	0.7
	Radial blanket 1				2.4442E+05	-0.4	1.2
	Radial blanket2	8.2701E+05	10.0	1.1	2.3004E+06	13.5	0.5
2	Core 1	2.5919E+08	-0.8	-0.6	3.9724E+08	1.0	0.5
	Core 2	1.3099E+08	-3.2	2.3	2.8833E+08	-1.9	0.0
	Radial blanket 1				6.5276E+06	-5.5	4.8
	Radial blanket2	2.5913E+07	5.2	0.0	6.1107E+07	9.2	0.5
3	Core 1	4.8042E+08	-0.8	-0.5	8.2092E+08	0.2	0.1
	Core 2	2.4780E+08	-1.5	-0.2	5.6565E+08	-1.2	-0.3
	Radial blanket 1				2.4652E+07	0.6	1.7
	Radial blanket2	6.3656E+07	2.1	-0.7	1.9432E+08	3.8	0.1
4	Core 1	7.5419E+08	-0.5	-0.3	1.3178E+09	-0.1	0.0
	Core 2	4.0113E+08	0.1	-0.1	8.9684E+08	-0.4	-0.2
	Radial blanket 1				6.0649E+07	1.5	0.7
	Radial blanket2	1.1709E+08	0.8	-1.0	4.1199E+08	2.0	0.3
5	Core 1	6.3882E+08	-0.1	0.0	1.0382E+09	-0.2	-0.0
	Core2	3.8159E+08	0.4	-0.2	7.1024E+08	-0.2	-0.2
	Radial blanket 1				8.0724E+07	1.8	0.7
	Radial blanket2	1.4044E+08	0.9	-0.7	3.7536E+08	1.5	0.1
6	Core 1	3.3921E+08	0.2	0.3	5.1874E+08	-0.3	-0.1
	Core 2	2.4290E+08	0.8	-0.2	3.6241E+08	-0.0	-0.2
	Radial blanket 1				7.5862E+07	1.8	0.6
	Radial blanket2	1.1813E+08	0.7	-0.6	2.3851E+08	1.2	0.1
7	Core 1	1.8130E+08	0.7	0.6	2.3454E+08	-0.4	-0.1
	Core2	1.4929E+08	1.2	-0.1	1.6657E+08	0.1	-0.1
	Radial blanket 1				5.9306E+07	1.6	0.4
	Radial blanket2	8.7010E+07	0.3	-0.8	1.2669E+08	1.2	0.1
8	Core 1	4.0238E+07	1.4	1.4	4.3344E+07	-0.4	-0.2
	Core 2	4.7220E+07	2.0	0.2	3.0712E+07	0.0	-0.2
	Radial blanket 1				2.9489E+07	1.5	0.3
	Radial blanket2	4.2219E+07	0.2	-0.8	3.3848E+07	1.3	0.0
9	Core 1	2.3783E+07	1.9	1.7	1.6426E+07	-0.4	-0.2
	Core 2	3.8886E+07	2.1	0.8	1.1807E+07	-0.0	-0.1
	Radial blanket 1				2.6332E+07	0.6	-0.2
	Radial blanket2	3.7395E+07	-0.4	-1.1	1.9556E+07	1.9	0.3
K-eff		1.12262	-0.54	-0.49	1.08329	-0.25	-0.09
CPU		1234.8	3.5	5.3	1264.6	3.6	4.6

1) Percent difference

One can find that the multiplication factors of TWOHEX are larger than those of the diffusion nodal calculations, and that is found in SNR problems consistently. The SP_2 nodal calculations reduced the errors of multiplication factors of diffusion nodal up to 50 %

except BFS-73-1. The error of the region-averaged fluxes was peaked at the radial blanket in the first or second groups in both calculations. But the maximum error of the region-averaged fluxes is remarkable reduced in the SP_2 nodal calculations, for example, the magnitude of the maximum errors are reduced to one third in the BFS-50's series.

5.3. LWR-LIKE BENCHMARK PROBLEMS

Although the numerical result of the SP_2 nodal described in the previous sections are very encouraging, it is doubtful that same or similar results are occurred in the light water reactors. Since light water reactors are analyzed by two group cross sections typically and the higher energy effects are negligible under the thermal spectrum environment, the advantage of the SP_2 theory may be faded out in the light water reactors. With these preconceptions, we calculated the various two-dimensional benchmark problems of light water reactors having a hexagonal geometry, e.g., IAEA problem,[18,19] VVER-440 problem,[20] and small size HTGR problem.[21] Here, for the convenience of calculations, we modified the small size HTGR problem having 60-degree reflective symmetry with vacuum boundary condition. Table VI shows the numerical result of these LWR-like problems.

Table VI. Summary of two-dimensional LWR-like benchmark problems

Core	k-effective value				Maximum error of region-ave. flux	
	TWOHEX	Diffusion[1)]	SP2[1)]	Ref.	Diffusion[1)]	SP2[1)]
IAEA without reflector.	0.98039	-0.02	0.09	0.97808[2)]	-4.8	-4.1
IAEA with reflector	1.00579	-0.36	-0.45	1.00551[2)]	-15.7	-17.7
VVER-440	1.01139	-0.33	-0.30	1.00970[3)]	-6.8	-10.6
HTGR fully rodded I	0.77339	-0.24	-0.10	-	-1.7	-2.3
HTGR fully rodded II	0.78176	-0.21	-.0.06	-	-1.7	-2.3
HTGR unrodded	0.99722	-0.31	-0.32	-	0.6	0.5

1) Percent difference
2) k-effective value of reference 19
3) k-effective value of reference 20

As contrasted with the SNR or BFS problems, we could not find any improvement of the accuracy in the SP_2 nodal calculations in these problems; neither the eigenvalues nor the region-averaged fluxes. These results were anticipated already. That is to say, the accuracy improvement of the SP_2 nodal was occurred principally at the non-dense or blanket regions with higher neutron energies, for examples, control rods, followers, and radial/axial blankets of Liquid Metal Rectors. At these circumstances, the transport effects become dominant and the diffusion theory has a poor accuracy. Therefore, we obtained the more accurate results at there by the SP_2 nodal than the diffusion nodal because the SP_2 nodal can catch up the transport effect in some degrees. However, in the LWR problems, there are few regions having a thin density and the transport effects of higher energy neutrons are already condensed into two groups data in the preparing the two group cross sections by using the high accurate lattice code.

6. CONCLUSION

In order to improve the accuracy of the diffusion nodal method, we developed an interface current nodal formulation for the solution of the multi-group SP_2 equations in hexagonal geometry. The nodal SP_2 equations have been incorporated as an option in the framework of the conventional nodal diffusion equations. By introducing the SP_2 factor α and the SP_2 flux ζ, we can formulate the nodal SP_2 equations with minimum modification of the conventional diffusion nodal equations and make it possible to use the conventional numerical schemes, such as fission source iteration accelerated by coarse-mesh rebalancing method. But, the relationship between the surface-averaged flux and the partial currents at the intra-node interfaces in the SP_2 approximations gives rise to additional term, i.e., the surface-averaged source term, in the response matrix equations. Numerical calculations were performed in two kinds of benchmark problems: LMR and LWR problems. Diffusion and SP_2 nodal results were compared by the reference S_n transport calculations in terms of the accuracy of multiplication factor, region-averaged flux distribution, and the computational effort. We found that the accuracies of the SP_2 nodal method were improved in the all kinds of the LMR problems. Especially, the SP_2 nodal solutions reduced the error of the multiplication factor up to 50 % and there are conspicuous improvements for

estimating the region-averaged fluxes in the non-dense or blanket regions with higher neutron energies, where the transport effects are dominant. However, in LWR problems, since there are no thin-density regions and the higher energy effect was already condensed when prepared the two-group cross sections, we could not find any improvement of the accuracy in the SP_2 nodal calculations. But because the SP_2 nodal equations require the computation of the surface-averaged sources additionally, the total computing time of the SP2 nodal was increased about 50% and that becomes a burden in the large size problems.

ACKNOWLEDGEMENT

This work was performed under Long-term Nuclear R & D Program sponsored by the Ministry of Science and Technology, R.O.K.

REFERENCES

1. E. M. Gelbard, " Application of Spherical harmonics Method to Reactor Problems," WAPD-BT-20 (1960).
2. E. M. Gelbard, "Simplified Spherical Equations and Their Use in Shielding Problems," WAPD-T-1182 (1961).
3. E. M. Gelbard, "Applications of the Simplified Spherical Harmonics Equations in Spherical Geometry," WAPD-TM-294 (1962).
4. Dorde Tomasevic, "The Simplified P_2 Correction to the Multi-dimensional Diffusion Equation," *Trans. Am. Nucl. Soc*., **66**, 232 (1992).
5. R. F. Gamino, "Simplified P_L Nodal Transport Applied to Two-Dimensional Deep-Penetration Problems," *Trans. Am. Nucl. Soc*., **59**, 149 (1983).
6. Miriam Lemanska, " On the simplified Pn Method in the 2-D diffusion Code EXTERMINATOR," *Atomkernenergie, Kerntechnik*, **37**, 173 (1981).
7. R. G. Gamino, "Three-Dimensional Nodal Transport Using The Simplified P_L Method," ANS topical meeting on Advances in Mathematics and computations and Reactor

Physics, April 29, Pittsburgh (1991).

8. Dorde Tomasevic, “Variational Derivation of Simplified P2 Equations with Boundary Conditions,” *Trans. Am. Nucl. Soc*., **70**, 159 (1994).
9. U. C. Shin, etc., “ The Time-Dependent Simplified P_2 Equations: Asymptotic Analyses and Numerical Experiments,” *Nucl. Sci. Eng*., **128**, 27 (1998).
10. E. W. Larsen, “Asymptotic Derivation of the Multigroup P_1 and SP_N Equations,” *Trans. Am. Nucl. Soc*., **69**, 209(1993)
11. E. W. Larsen, “Asymptotic Derivation of the Multigroup P_1 and Simplified P_N Equations with Anisotropic Scattering,” Int’l Conference on Mathematics and Computations Reactor Physics, and Environmental Analyses, April 30 – May 4, Portland (1995).
12. Young-In Kim, et al., “Nuclear and Thermal-hydraulic Characteristics for an LMR Core Fueled with 20% Enriched Uranium Metallic Fuel,” *Ann. Nucl. Energy*, **26**, 679 (1999).
13. J. D. Kim, et al., “KAFAX-F22: Development and Benchmark of Multi-group Library for Fast Reactor Using JEF-2.2,” KAERI/TR-842/97, Korea Atomic Energy Research Institute (1997).
14. R. D. Lawrence, “The DIF3D Nodal Neutronics Option for Two- and Three-Dimensional Diffusion Theory Calculation in Hexagonal Geometry,” ANL-83-1, Argonne National Laboratory (March, 1983).
15. W. S. Yang, “Response Matrix Properties and Convergence Implications for an Interface-Current Nodal Formulation,” *Nucl. Sci. Eng*., **121**, 416(1995)
16. Rudi J. J. Stamm’ler, “ Methods of Steady-State Reactor Physics in Nuclear Design,” Academic press (1983).
17. “Benchmark Problem Book,” ANL-7416, Supplement 3, Argonne National Laboratory (Dec. 1985).
18. “Benchmark Problem Book,” ANL-7416, Supplement 2, Argonne National Laboratory (Dec. 1977).
19. Y.A. Chao, “Benchmark Problems for Two Group Hexagonal Geometry Nodal Diffusion Codes,” Proceeding of International Conference on Mathematics and

Computations, Reactor Physics, and Environmental Analyses, Portland, Oregon, Vol. 2, 1233(1995).

20. F. Seidal, etc., “2-D and 3-D Diffusion Calculations for the VVER-440 Core Model,” 13th Symposium on Physics of VVER, Curtea de Agres, Romania (1984).
21. T. Y. C. Wei, “The Finite Element Method for Neutron Diffusion Problems in Hexagonal Geometry,” Ph.D. Thesis, M.I.T, (1975).
22. “Report on Results of Researched and Descriptions of BFS-51 and BFS-55 Critical Assemblies,” Institute of Physics and Power Engineering (1995).
23. “Report on Experimental Results on BFS-55-2 Critical Assembly,” Institute of Physics and Power Engineering (1998).
24. “Report on Results of Measurements on Benchmark Core of BFS-73-1 Critical Assembly,” Contract for Experimental Study on Metal Fueled Core Characteristics between KAERI and IPPE (1997).
25. “Report on Investigations of BFS-75 Critical Assembly,” Contract for Experimental Study of Characteristics of Core with Metal Fuel between KAERI and IPPE (1999).
26. W. F. Walters, etc., “User’s Guide for TWOHEX: A Code Package for Two-Dimensional, Neutral-Particle Transport in Equilateral Triangular Meshes,” LA-12969-M, Los Alamos National Laboratory (June, 1995).
27. M. R. Wagner, “Three-Dimensional Nodal Diffusion and Transport Theory Methods for Hexagonal-Z Geometry,” *Nucl. Sci. Eng*., **103**, 377(1989).
28. H. Khalil, etc., “ Performance of ANL Hexagonal Geometry Nodal Diffusion Methods,” *Trans. Am. Nucl. Soc*., **71**(1994).
29. MacFarlane, “TRANSX 2: A Code for Interfacing MATXS Cross-Section Libraries to Nuclear Transport Codes,” LA-12313-MS, Los Alamos National Lab.(1993).
30. H. Song, and T. K. Kim, et al., “Evaluation of Core Nuclear Analysis Code System for LMR using Measured Physics Parameters of BFS-73-1 Critical Assembly,” *Annals of Nuclear Energy,* **27**, 117(1999).